Annals of Nuclear Energy 98 (2016) 19–25

Contents lists available at ScienceDirect

Annals of Nuclear Energy

journal homepage: www.elsevier.com/locate/anucene

# A comparative study of Kalman filter and Linear Matrix Inequality based H infinity filter for SPND delay compensation

P.K. Tamboli [a,*], Siddhartha P. Duttagupta [a], Kallol Roy [b]

[a] Electrical Engineering Dept., Indian Institute of Technology Bombay, Mumbai, India
[b] CMD, BHAVINI, India

ARTICLE INFO

*Article history:*
Received 6 November 2014
Received in revised form 12 May 2016
Accepted 28 June 2016
Available online 26 July 2016

*Keywords:*
Kalman filters
Signal to Noise ratio
Minimax techniques

ABSTRACT

This paper deals with delay compensation of vanadium Self Powered Neutron Detectors (SPNDs) using Linear Matrix Inequality (LMI) based H-infinity filtering method and compares the results with Kalman filtering method. The entire study is established upon the framework of neutron flux estimation in large core Pressurized Heavy Water Reactor (PHWR) in which delayed SPNDs such as vanadium SPNDs are used as in-core flux monitoring detectors. The use of vanadium SPNDs are limited to 3-D flux mapping despite of providing better Signal to Noise Ratio as compared to other prompt SPNDs, due to their small prompt component in the signal. The use of an appropriate delay compensation technique has been always considered to be an effective strategy to build a prompt and accurate estimate of the neutron flux. We also indicate the noise-response trade-off curve for both the techniques. Since all the delay compensation algorithms always suffer from noise amplification, we propose an efficient adaptive parameter tuning technique for improving performance of the filtering algorithm against noise in the measurement.


## 1. Introduction

In Pressurised Heavy Water Reactors (PHWRs), the neutron flux distributed over the entire core does not provide an absolute value of reactor power. The neutron flux signal thus, heavily depends on the calibration with respect to some reference power sensed by other signals such as total thermal output of the core. Other factors such as reactivity device fluctuations, non-linear core model, uncertainty about reactivity information and sensor degradation worsen the overall situation. The reactor control or protection systems heavily rely upon the prompt and accurate information of neutronic flux for taking any control or safety action.

The detectors used for sensing the neutron or gamma flux are known as Self Powered Neutron Detectors (SPNDs). These are in-core instruments used for measuring neutron flux inside the reactor core and are primarily used for regulation and protection of the reactor. The neutron interacts with the SPND sensitive material and undergoes several transitions out of which some of the transitions are prompt while others are delayed depending upon the characteristics of the sensitive material. The term "delay" is generally used across the industries to represent the first order lag exhibited by the SPND output. The SPND based on n, $\beta$ such as vanadium is slow responding and its accuracy in terms of signal to noise ratio is relatively higher as compared to SPNDs based on n, $\gamma$, e. The use of vanadium SPNDs has been limited to less critical but important application such as online three dimensional flux mapping along the different geometric planes in the reactor core. Therefore, it is of much interest to develop a robust delay compensation algorithm for n, $\beta$ based SPNDs to make them useful for safety critical application.

A dynamic delay compensation technique to make use of these SPND signals into a more useful prompt signal has always been considered a good strategy. The most common delay compensation techniques initially used were based on direct inversion of the forward transfer function from input flux to the SPND current output and was introduced by Banda and Nappi (1976) for delay compensation of Rhodium SPND primarily used in Light Water Reactors (LWRs). The direct inversion technique provided a reasonable solution for SPND delay compensation; however, it is a well understood fact that this technique tends to increase the noise in the output signal if the measurement is affected by noise. The later researches in similar line were made to address the above issue by Yusuf and Wehe (1990) and Kulacsy and Lux (1997) by using analog techniques. The widespread development of the Kalman filters introduced by Kalman (1960) and later by Maybeck (1982) and Sorenson (1970), led to development of Kalman filter based delay compensation techniques which performed better than the direct

* Corresponding author.
*E-mail addresses:* pktamboli@iitb.ac.in (P.K. Tamboli), sdgupta@ee.iitb.ac.in (S.P. Duttagupta), kallolr@barc.gov.in (K. Roy).

http://dx.doi.org/10.1016/j.anucene.2016.06.033
0306-4549/

inversion technique in terms of noise in the final estimated output. The Kalman filter based solution can be found in Auh (1994) and Kantrowitz (1987). Some recent development in Kalman filter based delay compensation can be found in Srinivasarengan et al. (2012) and Mishra et al. (2013). The Kalman filter has limitation in terms of the knowledge of the noise characteristics and linearity and therefore the robust solutions based on $H_\infty$ filtering was proposed by Park et al. (1999) and the performance was further shown to be improved. However the essential problem of noise amplification has remained unsolved in all the previous research work which obstruct their used for many practical purposes. An adaptive technique based on the fading memory based $H_\infty$ was proposed in Tamboli et al. (2015) which adapts the rate of changes of measured signal unto fading memory forgetting factor. This technique produce much improved results however requires a parallel filter for filtering the noisy measurement and hence requires more computational effort.

The paper deals with two issues in general; first is the formulation for delay compensation along with the trade-off between noise and response time when using the delay compensation algorithms and second issue is the degradation in SNR associated with delay compensation algorithms. For the latter issue we propose the adaptive technique based on the dynamic tuning of the process covariance matrix. The proposed technique in a broad sense controls the filter parameter such that the contribution of delay compensation algorithm exists only when the need arises, reflected in terms of updated process covariance matrix. This way, the noise in the estimated output reduces to a minimum, under the steady state condition (i.e. in the absence of a transient) and the overall signal to noise ratio improves considerably. The proposed technique is less computational intensive as compared to other proposed method. The entire work is done primarily for vanadium SPND however the same can be readily extended to other SPNDs with more complex distribution of delayed fractions.

The paper is structured as follows: in Section 2, we describe the PHWRs in brief followed by the description of SPND and its working principle. In Section 3, we present the detailed derivation and study of the delay compensation methodology followed by simulation studies and the trade-off curves. In Section 4, we present the formulation for the adaptive delay compensation technique based on state difference, followed by the simulation studies. We also present off-line simulation experiments on the real time sensor data for demonstrating the performance of the proposed technique.

## 2. Pressurised Heavy Water Reactor (PHWR) model

The Pressurised Heavy Water Reactor (PHWR) is based on pressure tube concept with heavy water ($D_2O$) as both coolant and moderator. The core diameter is approximately 7 m and length is approximately 6 m. The detailed description of PHWR is beyond the scope of this paper; however a brief description is necessary before moving on to the flux estimation concepts. The reactor core dynamic behaviour is explained by the Point Kinetic Equations (PKEs) which are derived from the neutron transport equation involving neutron diffusion and generation. The PKEs describe the rate of change of neutron density ($n.cm^{-2}.sec^{-1}$) with respect to reactivity and delayed neutron precursor concentration. The point kinetic model can be written as (Tiwari et al., 1996):

$$\left.\begin{aligned}\frac{dN}{dt} &= \frac{(\rho-\beta_r)}{l}N + \sum_{r=1}^{6}\lambda_r C_r,\\ \frac{dC_r}{dt} &= \frac{\beta_r}{l}C_r - \lambda_r C_r,\end{aligned}\right\} \tag{1}$$

where $N$ is the neutron density (neutrons.cm$^{-3}$). $\beta_r$ and $\lambda_r$ denote the delayed neutron fractional yield and decay constant of the fission product neutron precursor group $r$. $C_r$ represent the concentration of the precursor group $r$ at time $t$. The expression for concentration of the precursor group can be replaced with average concentration $C$ replacing $\beta_r$ and $\lambda_r$ with their average $\beta$ and $\lambda$. $\rho$ denotes reactivity controlled by the reactivity devices.

The above model explains the behaviour for small core homogeneous model. For large core reactor, the point kinetic model can be expanded to multiple point kinetic equations each controlled by its associated reactivity device and coupled to each other through coupling coefficient as follows:

$$\left.\begin{aligned}\frac{dN_i}{dt} &= \frac{(\rho_i-\beta)}{l}N_i + \lambda C - \frac{1}{l}\sum_{j=1}^{n} m_{ij}N_i + \frac{1}{l}\sum_{j=1}^{n} m_{ji}N_j,\\ \frac{dC_i}{dt} &= \frac{\beta}{l}N_i - \lambda C,\end{aligned}\right\} \tag{2}$$

where $n$ is the number of cells affected by localized flux variation. Since we have used the normalized flux the $N_i$ is replaced with $N_i/N_F = N_i'$ and $C_i$ will be replaced with $C_i/N_T = C_i'$, where $N_T$ is the flux at full power (i.e. $2\times10^{14}$ nv). The coupling coefficient $m_{ij}$ can be given by:

$$\begin{aligned} m_{ij} &= \frac{Dvl\chi_{ij}}{d_{ij}V_j} \quad (i\neq j),\\ m_{ii} &= 0,\end{aligned} \tag{3}$$

where $D$ is the diffusion coefficient; $v$ is thermal neutron speed; $l$ is prompt neutron life time; $\chi_{ij}$ is the area of the interface between $i$th and $j$th zone; $d_{ij}$ the centre to centre distance between $i$th and $j$th zone and $V_j$ is volume of the $j$th zone. The coupling coefficient between a zone and a non-neighbouring zone can be conveniently assumed to be zero. The PKE is a set of stiff non-linear equation since the rate of neutron density variations heavily depends upon the reactivity. The proper zonal reactivity control can be only achieved through accurate and prompt neutron flux information.

### 2.1. Self Powered Neutron Detectors

The reactor power for large core PHWR cannot be accurately assessed by average flux information measured throughout core neutron flux sensors such as Ionization Chamber. The core condition for such cases is assessed by a number of in-core sensor i.e. self powered neutron detector. Various neutron or gamma sensitive material is used for sensing the in-core flux such as rhodium, cobalt, nickel, platinum or vanadium. The material based on $n,\gamma,e$ exhibits prompt response whereas material based on $n,\beta$ such as vanadium and Rhodium exhibits delayed response. The schematic of SPND is shown in the Fig. 1.

Among the above mentioned materials, the SPND with $n,\beta$ exhibits higher signal strength and hence provides better signal to noise ratio. Due to higher signal strength from vanadium SPND, they provide more accurate readings and are used as a reference to correct less accurate and prompt SPNDs.

The observation model is a first order linear dynamic model with $\phi_k$ as input and $y_k$ as measured output and can be written as

$$x_k = e^{-Ts/\tau}x_{k-1} + (1-e^{-Ts/\tau})\phi_{k-1} + w_{k-1} \tag{4}$$

$$y_k = (1-k_p)x_k + k_p\phi_k, \tag{5}$$

where $\tau$ = 325 s for vanadium SPND and $k_p$ is the prompt component fraction which is equal to 0.07. The above expression is normalised and brings the state and input vector to same dimensions and is useful for building the adaptive technique later discussed in the paper. The model can be generalised for the signal containing various components with different time constant $\{\tau_1,\tau_2\ldots\}$ and different proportion $\{k_1,k_2\ldots\}$. Fig. 2 shows the typical histogram for 50,000 data points of noise amplitude experimentally obtained for

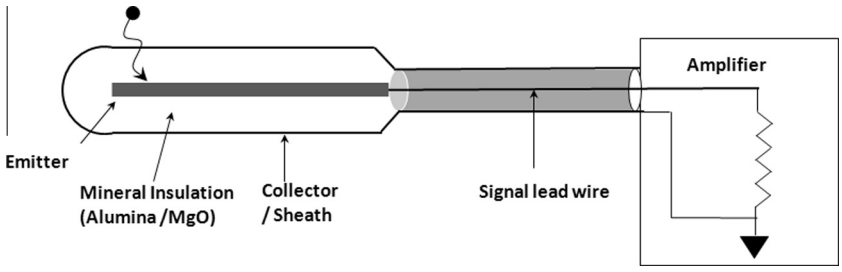


**Fig. 1.** Typical SPND schematic.

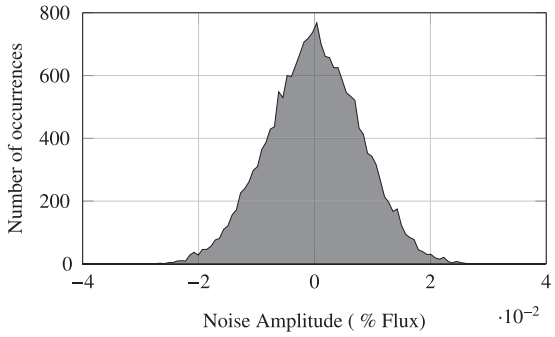


**Fig. 2.** Noise histogram of SPND.

an Inconel SPND of length 868 mm. The sampling interval was kept as 50 ms.

The above experiment provides direct information of noise variance and its characteristics. Null hypothesis test for confirming Gaussian distribution was performed before applying the algorithm. It was observed that the Gaussian distribution cannot be a generic nature for all SPNDs. Some SPNDs were observed to have skewed Gaussian distribution of noise.

## 3. Delay compensation algorithm

### 3.1. Augmented Kalman filter for delay compensation

The Kalman filter provides the analytical solution for the state estimation problem by minimizing the trace of estimation error covariance matrix i.e. $P_k$ for discrete time linear Gaussian dynamic system defined as (Welch and Bishop, 2006):

$$\mathbf{x}_{k+1} = A_k\mathbf{x}_k + B_k\mathbf{u}_k + \mathbf{w}_k \tag{6}$$

$$\mathbf{y}_k = C_k\mathbf{x}_k + D_k\mathbf{u}_k + \mathbf{v}_k, \tag{7}$$

where $\mathbf{x} \in \mathbb{R}^{n\times 1}$ is state vector to be estimated, $\mathbf{y} \in \mathbb{R}^{p\times 1}$ is measurement output vector, $\mathbf{u}_k \in \mathbb{R}^{m\times 1}$ is input vector. $\mathbf{w} \in \mathbb{R}^{n\times 1}$ and $\mathbf{v} \in \mathbb{R}^{m\times 1}$ are process and measurement disturbance vectors respectively. $A_k; B_k; C_k$ and $D_k$ are matrices of appropriate dimensions. For the time invariant model these matrices are constants. The Kalman filter algorithm requires knowledge of $Q_k$ and $R_k$, which are non-negative definite matrices representing process and measurement disturbance covariance matrices. $K_k$ is Kalman gain vector at $k$th instant. The Kalman filter recursive steps are written as

$$\mathbf{x}_{k+1}^{-} = A_k\mathbf{x}_k^{+} + B_k\mathbf{u}_k \tag{8}$$

$$P_{k+1}^{-} = A_kP_k^{+}A^T + Q_k \tag{9}$$

$$K_{k+1} = P_{k+1}^{-}C_{k+1}^T[C_{k+1}P_{k+1}^{-}C_{k+1}^T + R_{k+1}]^{-1} \tag{10}$$

$$P_{k+1}^{+} = (I - K_{k+1}C_{k+1})P_{k+1}^{-} \tag{11}$$

$$\mathbf{x}_{k+1}^{+} = \mathbf{x}_{k+1}^{-} + K_{k+1}(\mathbf{y}_{k+1} - C_{k+1}\mathbf{x}_{k+1}^{-} - D_{k+1}\mathbf{u}_{k+1}) \tag{12}$$

For a forced system, Kalman filter requires knowledge of the input vector. However in case of SPNDs with large delayed fraction, only a small component of signal provides the information about the prompt flux (forcing input) change. To compensate for large delayed portion of the signal, the unknown input is augmented in the state vector as another state variable with following hypothetical model.

$$\mathbf{u}_{k+1} = \mathbf{u}_k + \mathbf{n}_k, \tag{13}$$

where $\mathbf{n}_k \in \mathbb{R}^{m\times 1}$ is the disturbance vector, which is required for defining a large uncertainty term. The input vector is augmented to state vector increasing the overall order of the filter. The augmented model can be described as:

$$\begin{bmatrix}\mathbf{x}_{k+1}\\ \mathbf{u}_{k+1}\end{bmatrix} = \begin{bmatrix}A_k & B_k\\ 0 & 1\end{bmatrix}\begin{bmatrix}\mathbf{x}_k\\ \mathbf{u}_k\end{bmatrix} + \begin{bmatrix}\mathbf{w}_k\\ \mathbf{n}_k\end{bmatrix} \tag{14}$$

$$\mathbf{y}_k = [\,C_k \quad D_k\,]\begin{bmatrix}\mathbf{x}_k\\ \mathbf{u}_k\end{bmatrix} + \mathbf{v}_k \tag{15}$$

or

$$\tilde{\mathbf{x}}_{k+1} = A_k'\tilde{\mathbf{x}}_k + \tilde{\mathbf{w}}_k \tag{16}$$

$$\mathbf{y}_k = C_k'\tilde{\mathbf{x}}_k + \tilde{\mathbf{v}}_k, \tag{17}$$

where $\tilde{\mathbf{x}}_k \in \mathbb{R}^{(n+m)\times 1}$ is augmented state vector. The Kalman filter recursion can now be applied to the augmented model for the estimation of both the state. The state variable defined for unknown input is estimated in this process and appear as delay compensated output. The augmented model considering unknown % flux input as another state variable can be written as:

$$\begin{bmatrix}x_{k+1}\\ \phi_{k+1}\end{bmatrix} = \begin{bmatrix}e^{-Ts/\tau} & 1-e^{-Ts/\tau}\\ 0 & 1\end{bmatrix}\begin{bmatrix}x_k\\ \phi_k\end{bmatrix} + \begin{bmatrix}w_k^1\\ w_k^2\end{bmatrix} \tag{18}$$

$$y_k = \begin{bmatrix}1-k_p & k_p\end{bmatrix}\begin{bmatrix}x_k\\ \phi_k\end{bmatrix} + v_k \tag{19}$$

The Kalman filter assumes the uncertainties to be Gaussian, however this may not be the case always in real life situation. For such cases the Kalman filter still provide minimum error variance but does not guarantees the unbiased estimates (Chen et al., 2004).

### 3.2. LMI-based a priori augmented $H\infty$ filter

The limitations of Kalman filter for non-Gaussian uncertainty can be solved by using robust estimation techniques i.e. $H_\infty$ filtering method. The $H_\infty$ filtering also known as minimax filtering does not require probabilistic knowledge of the uncertainty or disturbance. It minimizes the maximum singular value of the matrix valued transfer function from disturbance input vector to estimation error vector. The $H_\infty$ filtering finds an estimate of the $\mathbf{x}_k$, which

minimizes the worst-case estimation error energy $\|e\|_2$ for all bounded energy disturbance $\|\omega\|_2$ (Yaesh and Shaked, 1991) i.e.

$$\min \sup_{\omega \in \mathcal{L}_2[0,\infty)} \|H_{\omega e}(je)\|_\infty < \gamma^2 \tag{20}$$

where $\|H_{\omega e}(je)\|_\infty$ is the transfer function from disturbance $\omega_k$ to the estimation error $\mathbf{e}_k$. The linear discrete time augmented model defined in Eqs. (16) and (17) can be written in an augmented form

$$\tilde{\mathbf{x}}_{k+1} = A'_k \tilde{\mathbf{x}}_k + B'_k \tilde{\omega}_k \tag{21}$$

$$\mathbf{y}_k = C'_k \tilde{\mathbf{x}}_k + D'_k \tilde{\omega}_k, \tag{22}$$

where

$$B'_k = \begin{bmatrix} B_k^1 & 0 & 0 \\ 0 & B_k^2 & 0 \end{bmatrix}_{(n+m)\times(n+m+p)} \tag{23}$$

$$D'_k = [\,0 \quad 0 \quad D_k\,]_{p\times(n+m+p)}. \tag{24}$$

$\tilde{\omega}_k \in \mathbb{R}^{(n+m+p)\times 1}$ can be considered to be an augmented disturbance vector consisting of three uncorrelated disturbance vectors $\omega_k^1, \omega_k^2$ and $\omega_k^3$. Each disturbance signal (vector valued) is defined as having unit covariance matrix.

$$E\{(\omega_k^i)(\omega_k^i)^T\} = I \quad \text{for } i = 1,2 \text{ and } 3 \tag{25}$$

The disturbance error vectors defined in Eqs. (16) and (17) can be related with disturbance vector $\tilde{\omega}_k$ as

$$\begin{bmatrix} \mathbf{w}_k \\ \mathbf{n}_k \end{bmatrix} = B'_k \tilde{\omega}_k \tag{26}$$

$$\mathbf{v}_k = D'_k \tilde{\omega}_k \tag{27}$$

The discrete time estimator has the following form:

$$\hat{\tilde{\mathbf{x}}}_{k+1} = A'_k \hat{\tilde{\mathbf{x}}}_k + A'_k K_k (\mathbf{y}_k - C'_k \hat{\tilde{\mathbf{x}}}_k) \tag{28}$$

The estimation error dynamic is given by

$$\mathbf{e}_{k+1} = (A'_k - K_k C'_k)\mathbf{e}_k + (B'_k - K_k D'_k)\tilde{\omega}_k \tag{29}$$

The discrete time Bounded Real Lemma for $\gamma$ stability for Eq. (29) can be written as (Park et al., 1999)

$$\begin{bmatrix} P & 0 & A_k'^T P - C_k'^T W^T & I \\ 0 & \gamma^2 I & B_k'^T P - D_k'^T W^T & 0 \\ PA'_k - WC'_k & PB'_k - WD'_k & P & 0 \\ I & 0 & 0 & I \end{bmatrix} > 0 \tag{30}$$

$$P > 0 \tag{31}$$

where $K_k = P^{-1}W$. The optimal $H_\infty$ filter is obtained by solving the LMI optimization problem subject to the LMI constraints above. The above LMI can be solved iteratively. A filter gain $K_k$ is obtained and can be applied to the filter equation. In this setting, the augmented model can be again written as

$$\begin{bmatrix} x_{k+1} \\ \phi_{k+1} \end{bmatrix} = \begin{bmatrix} e^{-Ts/\tau} & 1 - e^{-Ts/\tau} \\ 0 & 1 \end{bmatrix} \begin{bmatrix} x_k \\ \phi_k \end{bmatrix} + \begin{bmatrix} b1 & 0 & 0 \\ 0 & b2 & 0 \end{bmatrix} \begin{bmatrix} \omega_k^1 \\ \omega_k^2 \\ \omega_k^3 \end{bmatrix} \tag{32}$$

$$y_k = \begin{bmatrix} 1 - k_p & k_p \end{bmatrix} \begin{bmatrix} x_k \\ \phi_k \end{bmatrix} + \begin{bmatrix} 0 & 0 & d \end{bmatrix} \begin{bmatrix} \omega_k^1 \\ \omega_k^2 \\ \omega_k^3 \end{bmatrix} \tag{33}$$

where $\omega^1, \omega^2$ and $\omega^3$ are the uncorrelated disturbance input signal each one of them being zero mean white Gaussian noise with unit intensity. Since the expression for input matrices $B'$ and $D'$ for disturbances input is analogous to process and measurement error covariances $Q$ and $R$ in Kalman filter they can be related as The process and measurement error covariance matrices can be related as:

$$Q_{(n+m)\times(n+m)} = B'B'^t \tag{34}$$

$$R_{p\times p} = D'D'^t \tag{35}$$

Choosing a large value for $Q(2,2)$ element is equivalent to choosing large value of $B_{2,1}$ term.

### 3.3. Simulation studies for delay compensation (using fixed value of fictitious process noise)

To compare the performance of both filtering techniques for delay compensation under worst case (i.e. assuming the prompt fraction in both signal and the estimator model is zero), we apply a step change at the input to vanadium SPND model using both the techniques. The model uncertainty or process covariance matrix is defined as; $Q = \begin{bmatrix} 0.1 & 0 \\ 0 & 10^2 \end{bmatrix}$, where a value of $10^2$ for $Q(2,2)$ term has been used to define the model uncertainty for the assumed model for input flux. A small measurement noise equal to the real time noise obtained experimentally in Section 2.1 was added to the measurement i.e. $R = [0.1]$. The equivalent $B'$ and $D'$ matrices for the $H_\infty$ model are defined as

$$B' = \begin{bmatrix} \sqrt{Q(1,1)} & 0 & 0 \\ 0 & \sqrt{Q(2,2)} & 0 \end{bmatrix} \tag{36}$$

$$D' = [0, 0, \sqrt{R}] \tag{37}$$

We use the two standard parameters for comparing the performance of the filter. One is the "response time" defined as the time to reach 90% of the final value for a step change at the input. Second parameter the "Root Mean Square (RMS) value of the noise signal" calculated from the steady state variance in the estimated flux signal when there is. All the values used for calculations are normalised in percentage with respect to the full or rated power of the core.

#### 3.3.1. Without prompt fraction

The worst case scenario for any delay compensation technique is when no prompt fraction is observed at the measured output ($k_p$ = 0%) and the same is used inside the Kalman filter formulation. We conduct the simulation for this case first and the results are plotted in Fig. 3 for both the techniques. The response time of the filter can be defined in terms of estimated output as the time to reach 90% of its final value. It can be seen that for the assumed fictitious value of process noise covariance ($Q(2,2)$), the response time is typically 26 s. However the noise during the estimation has been increased due to the high filter gain.

#### 3.3.2. With prompt fraction

Another set of simulations are performed to study the performance of both the techniques with respect to different prompt fraction assuming the prompt fraction is exactly known and has been considered while developing the estimator. It is to be noted that if smaller prompt fraction is used in the model while the actual prompt fraction in the signal is large, it will result in large overshoots and undershoot in the opposite case.

It is expected that with the increase of prompt fraction the response of the delay compensation algorithm is improved i.e. it reduces the response time as well as improves the SNR. The normalised noise RMS and response time verses different prompt fraction is shown in Fig. 4 for $H_\infty$ filter and in Fig. 5 for Kalman filter. The black line shows response time in seconds and grey line shows

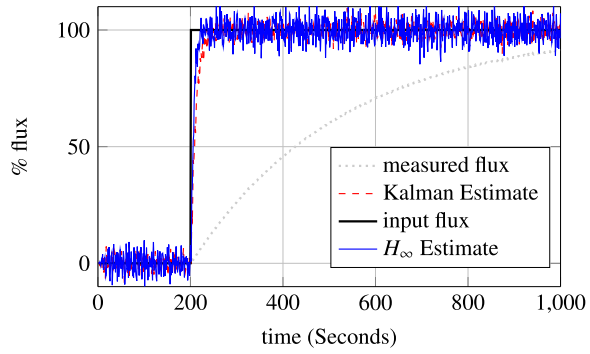


**Fig. 3.** Kalman filter based delay compensation for vanadium SPND signal: 0% prompt fraction.

normalised RMS noise. The smallest response time obtained for 10% prompt fraction is 1 s.

The steady state filter gain matrix $K$ in Eq. (28) for vanadium SPND has two components, i.e. $K(1,1)$ and $K(2,2)$. These are plotted to demonstrate the effect on filter gain of different prompt fraction in Fig. 6. It can be observed that filter gains decreases for large prompt fraction since less weight is required to be given to measurement to compensate for the delay. Another observation can be made with respect to $H_\infty$ filter that filter gain is usually higher resulting in lower response time as well as higher noise.

The noise RMS value in case of $H_\infty$ filter based delay compensation is determined by the fictitious noise value $Q(2,2)$ and performance bound $\gamma$.

### 3.3.3. The noise-response trade-off

The large filter gain decreases response time at the same time increases noise gain or estimation error variance under steady state. It can be therefore understood that, a trade-off exists between the response time verses noise RMS gain. The trade-off for both the filters hence can be created as one useful selection criteria before applying the delay compensation. Since $H_\infty$ filtering has an additional tuning parameter $\gamma$, multiple trade-off curves pertaining to various $\gamma$ values can be obtained.

The trade-off curves can be used to compare the two filters. The simulation results presented in this report are for vanadium SPND however similar trade-off curves and performance curves can be

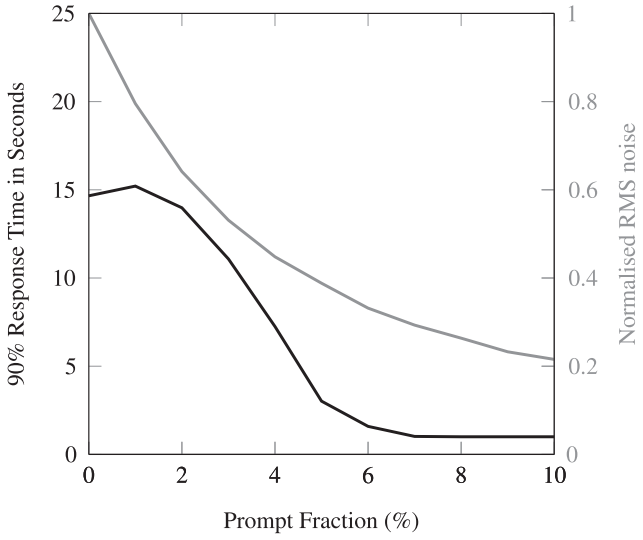


**Fig. 4.** Effect of prompt fraction: $H_\infty$ filter ($\gamma = 20,000$).

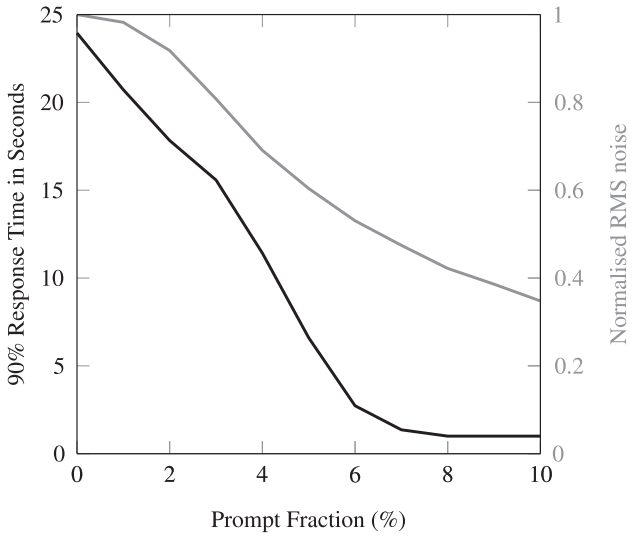


**Fig. 5.** Effect of prompt fraction: Kalman filter.

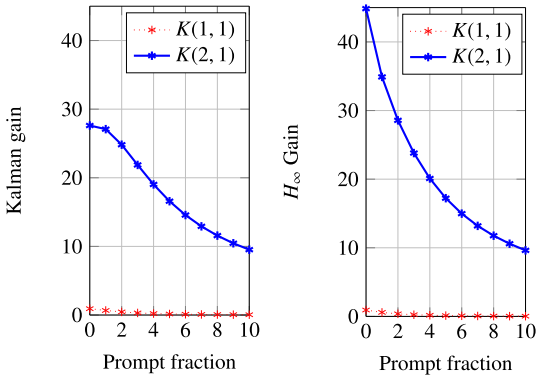


**Fig. 6.** Filter gain $K(1,1)$ and $K(2,1)$ variation with prompt fraction.

evaluated for other types of SPNDs with delayed components e.g. rhodium, platinum etc. The trade-off curve for Kalman filter based delay compensation is shown in Fig. 7. Similar trade-off curves for $H_\infty$ filter based delay compensation is shown in Fig. 8 for $\gamma$ values of $1.5 \times 10^4$ (solid lines), $2 \times 10^4$ (dashed lines) and $2 \times 10^5$ (dotted lines). The RMS noise plotted in both the figures are absolute values of the high frequency components of the estimated output. It is to be noted from the observation that, as the $\gamma$ value tends to $\infty$, the response of $H_\infty$ filter becomes similar to Kalman filter.

The trade-off curves show that, for lower $\gamma$ (stricter performance bound), the overall response time achieved by the $H_\infty$ filter are lower at the same time, RMS noise values are higher as compared to Kalman filter. The additional tuning parameter $\gamma$ in $H_\infty$ provides better adjustability from the application point of view.

## 4. Adaptive $H_\infty$ delay compensation based on the state difference

The problem of noise increase during all type of delay compensation techniques is well understood phenomenon and becomes very severe if measurement has unknown glitches (anomaly). The main factor responsible for increase in noise is high filter gain applied to innovation for the augmented state (input flux). The high filter gain is a results of high fictitious noise variance defined in delay compensation algorithm, which is selected arbitrary.

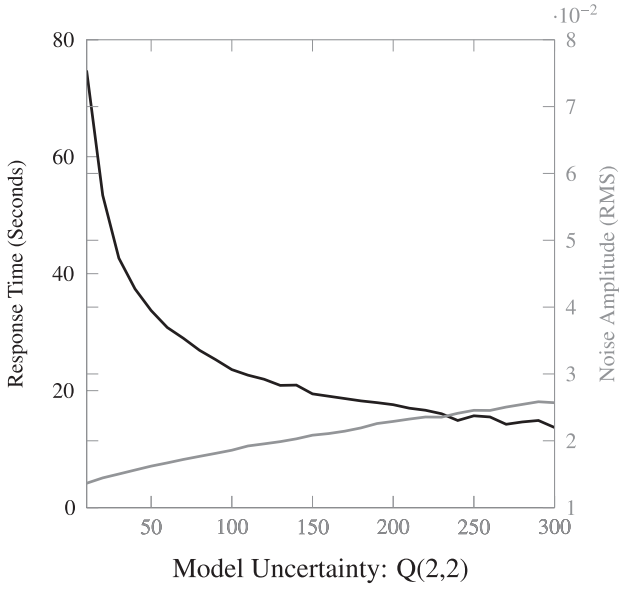


**Fig. 7.** Trade-off curve for Kalman filter.

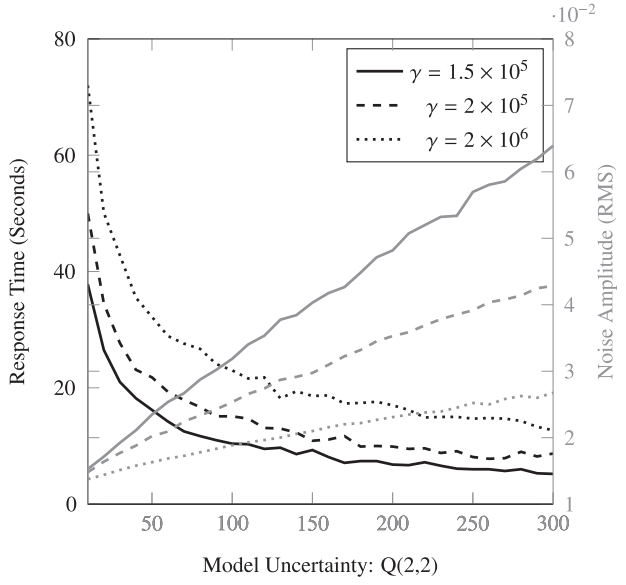


**Fig. 8.** Trade-off curve for $H_\infty$ filter.

In place of selecting the high process noise arbitrary, we propose a different solution based on adaptive parameter tuning to improve the steady state noise at the same time maintaining the response time. In this approach, the information contained in the estimated states during every state is exploited to generate process noise variance information. It should be noted that the SPND model can be represented in many different ways, however the state space representation in Eqs. (4) and (5) normalises the two states on the same scale and the parameter proportional to their difference can be calculated.

The adaptive technique requires calculation of filter gain at each instant. The LMI based $H_\infty$ filter is quite computation intensive and might not be suitable in this case. We use here a simpler recursive $H_\infty$ filtering technique similar to Kalman filter's recursion explained in Simon (2006) and Banavar and Speyer (1991). For the augmented model explained in Eqs. (16) and (17), the $H_\infty$ recursion can be written as

$$\hat{\tilde{\mathbf{x}}}_{k+1}^{-} = A_k' \hat{\tilde{\mathbf{x}}}_k^{+} \tag{38}$$

$$P_{k+1}^{-} = A_k' P_k^{+} A_k'^{T} + Q_k \tag{39}$$

$$K_{k+1} = P_{k+1}^{-}\left[I - \frac{1}{\gamma^2} S_k P_{k+1}^{-} + C_k'^{T} R^{-1} C_k' P_{k+1}^{-}\right]^{-1} C_k'^{T} R_k^{-1} \tag{40}$$

$$\hat{\tilde{\mathbf{x}}}_{k+1}^{+} = \hat{\tilde{\mathbf{x}}}_{k+1}^{-} + K_{k+1}(\mathbf{y}_{k+1} - C_k' \hat{\tilde{\mathbf{x}}}_{k+1}^{-}) \tag{41}$$

$$P_{k+1}^{+} = P_{k+1}^{-}\left[I - \frac{1}{\gamma^2} S_k P_{k+1}^{-} + C_k'^{T} R_k^{-1} C_k' P_{k+1}^{-}\right]. \tag{42}$$

The above set of equations provide an upper bound $\gamma$ on the following cost function.

$$J = \frac{\sum_{k=0}^{N-1} \|\tilde{\mathbf{x}}_k - \hat{\tilde{\mathbf{x}}}_k\|_{S_k}^2}{\|\tilde{\mathbf{x}}_0 - \hat{\tilde{\mathbf{x}}}_0\|_{P_0^{-1}}^2 + \sum_{k=0}^{N-1} (\|\mathbf{w}_k\|_{Q_k^{-1}}^2 + \|\mathbf{v}_k\|_{R_k^{-1}}^2)} < \gamma^2. \tag{43}$$

When all the states are given equal weight, the matrix $S_k$ can be assumed to be Identity matrix. Keeping our discussion limited to vanadium SPND model with two state variables, the process can be explained as follows: as the measurement variation starts to appear, the normalised value of the two states also start differing. At this point the model uncertainty $Q_k(2,2)$ is made to differ proportionately with the difference between the two estimated states. The increase in the model uncertainty value results into increased filter gain, which further increases the value of estimated flux input. After a few step when the model uncertainty reaches its peak, the estimated flux becomes almost equal to true flux. The model uncertainty starts decreasing beyond this point. We can introduce a factor $\theta$, which is proportional to the difference between the estimated states at every instant:

$$\theta_k = (\hat{x}_k - \hat{\phi}_k)^2 \tag{44}$$

The process noise covariance matrix $Q_k$ during $k$th can be related with $\theta_k$ at each instant as follows:

$$Q_k = \begin{bmatrix} Q(1,1) & 0 \\ 0 & \alpha + \beta\theta_k \end{bmatrix}, \tag{45}$$

where $Q(1,1)$ is the model uncertainty defined for the first state and is a fixed value. The unknown model uncertainty $Q(2,2)$ is replaced with an equation relating the state difference at each point. $\beta$ is a constant defined for controlling the response time and can be considered as learning or sensitivity parameter for the state difference. $\alpha$ is another term required for defining a minimum variance term and also sets the minimum steady state noise variance when there is no variation in signal.

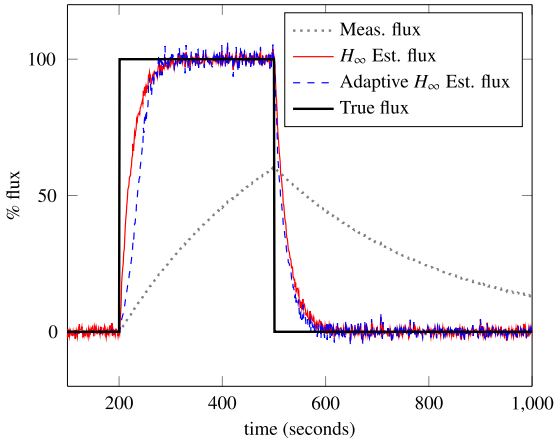


**Fig. 9.** Simulation Results for adaptive $H_\infty$ filtering for $\alpha = 1$.

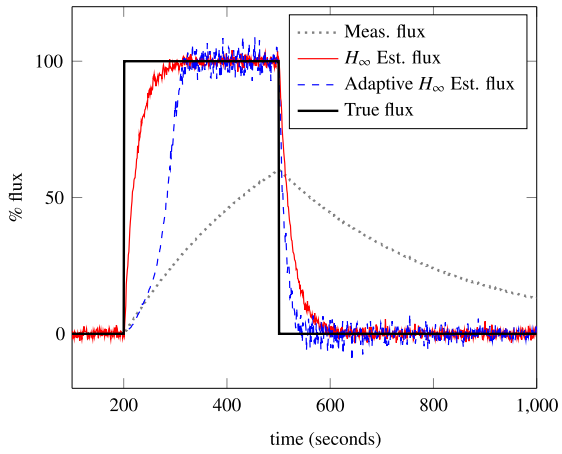


**Fig. 10.** Simulation Results for adaptive $H_\infty$ filtering for $\alpha = 0$.

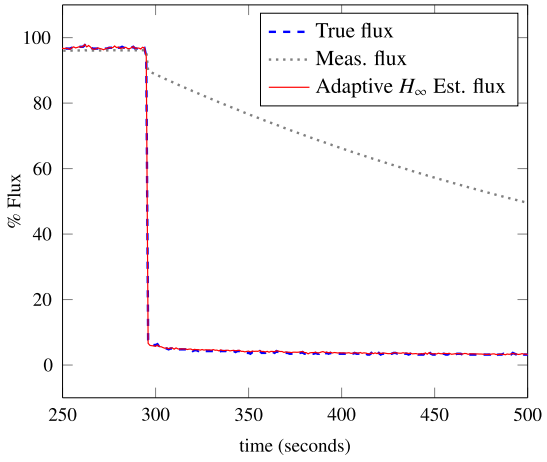


**Fig. 11.** Results of adaptive $H_\infty$ delay compensation on vanadium SPND during reactor trip.

### 4.1. Simulation studies for adaptive $H_\infty$ delay compensation

The performance of the adaptive dynamic filtering is shown in Fig. 9. The minimum variance $\alpha$ and sensitivity factor $\beta$ were kept as 1. The maximum variance during the step change is obtained in simulation is 150.

It can be seen that the adaptive filter reduces the steady state noise variance much effectively for the same response time. However the plot shows an increase in noise for the short duration during transient, which can be reduced to certain extent by more tuning. The important role played by $\alpha$ during the beginning of the transient can be seen in Fig. 10 where $\alpha$ is made zero. To demonstrate the performance of adaptive delay compensation algorithm developed, we conducted an off-line experiment using real time sensor data recorded from 540 MWe PHWR with scanning rate of 1 s. The reactor trip data was used to test the promptness achieved by the proposed method since fasted rate if flux change can be observed during reactor trip. The vanadium SPND signal was captured from SPND amplifier and a recorder that converts the raw signal into normalised flux value with respect to full power. The parameter $\alpha$ and $\beta$ were chosen as 10 for applying a higher initial rate and sensitivity. The plot in Fig. 11 shows that the response time achieved by using the adaptive filter is 10 s along with very low noise under steady state.

## 5. Conclusion

In this paper, we have presented a study that compares the Kalman filter based approach and $H_\infty$ filter based approach with respect to delay compensation of SPNDs. The results indicate that although both the method can be modified to build a suitable delay compensation algorithm, the $H_\infty$ due to its strict upper bound on performance, results into higher filter gain and provides a lower response time with slightly increase noise. We have built the trade-off curves for both the technique that makes the selection process much simpler for choosing the parameters. The recursive implementation and more number of tuning parameters makes the $H_\infty$ a better choice. We also propose the adaptive technique for $H_\infty$ filtering based delay compensation, which reduces the steady state noise significantly. The results were simulated for real time sensor data during reactor trip from full power and show that the SPND with adaptive delay compensation can become a good alternative with respect to better SNR as compared to the prompt SPNDs.

## References

Auh, G.-S., 1994. Digital dynamic compensation methods of rhodium self-powered neutron detector. Nucl. Eng. Technol. 26 (2), 205–211.
Banavar, R.N., Speyer, J.L., 1991. A linear-quadratic game approach to estimation and smoothing. American Control Conference, 1991. IEEE, pp. 2818–2822.
Banda, L., Nappi, B., 1976. Dynamic compensation of rhodium self powered neutron detectors. IEEE Trans. Nucl. Sci. 23 (1), 311–316.
Chen, W.-s., Bakshi, B.R., Goel, P.K., Ungarala, S., 2004. Bayesian estimation via sequential monte carlo sampling: unconstrained nonlinear dynamic systems. Ind. Eng. Chem. Res. 43 (14), 4012–4025.
Kalman, R.E., 1960. A new approach to linear filtering and prediction problems. J. Fluids Eng. 82 (1), 35–45.
Kantrowitz, M., 1987. An improved dynamic compensation algorithm for rhodium self-powered neutron detectors. IEEE Trans. Nucl. Sci. 34 (1), 562–566.
Kulacsy, K., Lux, I., 1997. A method for prompt calculation of neutron flux from measured spend currents. Ann. Nucl. Energy 24 (5), 361–374.
Maybeck, P.S., 1982. Stochastic Models, Estimation, and Control, vol. 3. Academic press.
Mishra, A.K., Shimjith, S., Bhatt, T.U., Tiwari, A.P., 2013. Dynamic compensation of vanadium self powered neutron detectors for use in reactor control. IEEE Trans. Nucl. Sci. 60 (1), 310–318.
Park, M.-G., Kim, Y.-H., Cha, K.-H., Kim, M.-K., 1999. $h\infty$ filtering for dynamic compensation of self-powered neutron detectors-a linear matrix inequality based method. Ann. Nucl. Energy 26 (18), 1669–1682.
Simon, D., 2006. Optimal State Estimation: Kalman, H Infinity, and Nonlinear Approaches. John Wiley & Sons.
Sorenson, H.W., 1970. Least-squares estimation: from gauss to kalman. IEEE Spectrum 7 (7), 63–68.
Srinivasarengan, K., Mutyam, L., Belur, M.N., Bhushan, M., Tiwari, A.P., Kelkar, M.G., Pramanik, M., 2012. Flux estimation from vanadium and cobalt self powered neutron detectors (spnds): nonlinear exact inversion and kalman filter approaches. American Control Conference (ACC), 2012. IEEE, pp. 318–323.
Tamboli, P.K., Duttagupta, S.P., Roy, K., 2015. Adaptive fading memory filter design for compensation of delayed components in self powered flux detectors. IEEE Trans. Nucl. Sci. 62 (4), 1857–1864.
Tiwari, A., Banyopadhyay, B., Govindarajan, G., 1996. Spatial control of a large pressurized heavy water reactor. IEEE Trans. Nucl. Sci. 43 (4), 2440–2453.
Welch, G., Bishop, G., 2006. An Introduction to the Kalman Filter. University of North Carolina, Chapel Hill, North Carolina, US.
Yaesh, I., Shaked, U., 1991. $h\infty$-optimal estimation: the discrete time case. Proc. Inter. Symp. on MTNS, pp. 261–267.
Yusuf, S.O., Wehe, D.K., 1990. Analog and digital dynamic compensation techniques for delayed self-powered neutron detectors. Nucl. Sci. Eng. 106 (4), 399–408.